PAUL SCHERRER INSTITUT

PSI-PR-96-34
Oktober 1996

sw9647

Experimental Determination of the Kinetic Energy Distribution of $\pi^- p$ Atoms in Liquid Hydrogen

A. Badertscher[b], M. Daum[a], R. Frosch[a], P. F. A. Goudsmit[b], W. Hajdas[a], M. Janousch[b], P.-R. Kettle[a], V. Markushin[a], J. Schottmüller[a,c], and Z. G. Zhao[b]

a Paul Scherrer Institut, PSI, CH-5232 Villigen PSI, Switzerland
b Institut für Teilchenphysik der ETHZ, IPP, CH-5232 Villigen PSI, Switzerland
c Physik-Institut der Universität Zürich, Winterthurerstrasse 190, CH-8057 Zürich, Switzerland

Paul Scherrer Institut
CH - 5232 Villigen PSI
Telefon 056 310 21 11
Telefax 056 310 21 99

Experimental determination of the kinetic energy distribution of $\pi^- p$ atoms in liquid hydrogen

A. Badertscher[2], M. Daum[1], R. Frosch[1], P. F. A. Goudsmit[2], W. Hajdas[1], M. Janousch[2], P.-R. Kettle[1], V. Markushin[1], J. Schottmüller[1,3], and Z. G. Zhao[2]

October 3, 1996

[1]PSI, Paul-Scherrer-Institut, CH-5232 Villigen-PSI, Switzerland

[2]IPP, Institut für Teilchenphysik der ETHZ, CH-5232 Villigen-PSI, Switzerland

[3]Physik-Institut der Universität Zürich, Winterthurerstr. 190, CH-8057 Zürich, Switzerland

E-mail address: Manfred.Daum@PSI.CH

Tel.: +41 56 310 36 68; Fax: +41 56 310 32 94

Abstract

We have investigated the kinetic energy distribution of $\pi^- p$ atoms in liquid hydrogen by measuring the Doppler broadening of neutron time-of-flight spectra from the reaction $\pi^- p \to \pi^0 n$. The existence of 'high energy' ($\gg 1\,\mathrm{eV}$) components, containing about half of the $\pi^- p$ atoms, is confirmed and evidence for discrete peaks with energies up to $\simeq 200\,\mathrm{eV}$ is found.

PACS: 36.10.Gv, 25.80.Fm, 13.75.Gx

In a previous experiment [1] in which the pion mass difference $m_{\pi^-} - m_{\pi^0}$, was determined from time-of-flight (TOF) of neutrons emitted in the charge-exchange (CEX) reaction $\pi^- p \to \pi^0 n$ in liquid hydrogen, we found a large fraction of 'high-energy' ($\gg 1\,\mathrm{eV}$) pionic atoms which led to a broadening of the neutron TOF peak; the observed broadening increased with the flight distance of the neutrons. Evidence for such 'high-energy' components was also reported in an experiment performed in hydrogen gas [2]. This Doppler broadening is related to the kinetic energy distribution $f(T_{\pi p})$ of $\pi^- p$ atoms at the instant of the CEX-reaction.

The distribution $f(T_{\pi p})$ can be used to test the cross-sections predicted for the various processes occurring during the cascade of exotic hydrogen atoms. Furthermore, a precise knowledge of the kinetic energy of the pionic hydrogen atoms during the cascade is important for other experiments, e.g. for the determination of the strong interaction width of the ground state in pionic hydrogen from a measurement of the pionic $(3P - 1S)$ X-ray transition [3]. Neutron time-of-flight experiments such as those described in Refs. [1, 2] are sensitive only to atomic states which decay by nuclear capture (mainly nS-states); it is left to cascade calculations to give predictions of kinetic energy distributions of pionic atoms in specific states, such as the $3P$-state [4].

The Doppler broadening of the TOF spectra observed [1, 2] can, at present, be attributed to one cascade process only, namely that of Coulomb de-

excitation [5] $(\pi^- p)_n + p \rightarrow (\pi^- p)_{n'} + p$ [1]. In this process an excited pionic atom collides with a proton of the surrounding hydrogen, causing a transition of the pionic atom. The de-excitation energy associated with the transition is then shared between the collision partners as kinetic energy. Other cascade processes, such as elastic scattering of non-thermalized pionic atoms and external Auger de-excitation, either reduce the kinetic energy $T_{\pi p}$ or leave it almost unchanged [2].

The rates of the Coulomb de-excitation process calculated by several authors [5, 7, 8, 9] disagree by more than one order of magnitude. Hence, precise data are needed to test the different predictions.

If one assumes that a $\pi^- p$ atom with negligible kinetic energy collides with a free proton, the kinetic energy of the $\pi^- p$ atom after a Coulomb de-excitation is given by

$$T_{\pi p} = \Delta E_{n,n'}/(1 + M_{\pi p}/m_p). \tag{1}$$

Here $\Delta E_{n,n'}$ is the energy difference of the two atomic states n and n', $M_{\pi p}$ and m_p are the masses of the $\pi^- p$ atom and the proton, respectively.

An idealized energy distribution $f(T_{\pi p})$ [10] with discrete peaks from the

[1] It is not excluded that the Coulomb de-excitation is part of some new mechanism, e.g. the formation of a resonant state, as was suggested for $n = 2$ [6].

[2] The possibility of a moderate acceleration in Auger de-excitation is discussed in Ref. [7].

Coulomb de-excitation mechanism, is shown in Fig. 1. In this distribution only transitions with $n' = n - 1$ are considered; according to Ref. [5] transitions with $\Delta n > 1$ are strongly suppressed. The low energy part of $f(T_{\pi p})$ is approximated by a uniform distribution between 0 and T_1. According to the kinematical formulae given in Ref. [11], the $T_{\pi p}$-distribution of Fig. 1a leads to the step-like neutron TOF distribution shown in Fig. 1b. The time variable τ is the difference of the neutron TOF (t) from the mean TOF (t_0). The rectangular TOF distributions in Fig. 1b correspond to the δ-like peaks in $f(T_{\pi p})$ shown in Fig. 1a, whereas the triangular distribution peaked at $\tau = 0$ corresponds to the uniform kinetic energy distribution extending from 0 to T_1. The area $A_{nn'}$ in Fig. 1b gives the relative probability for a $\pi^- p$ atom to undergo the Coulomb de-excitation transition $n \to n'$, which would result in a neutron TOF τ in the range $-\tau_{nn'} \leq \tau \leq +\tau_{nn'}$. The times τ_1 and $\tau_{nn'}$ in Fig. 1b are related to the kinetic energies T_1 and $T_{nn'}$ as follows:

$$\tau_1 = \frac{l}{v_0^2} \cdot \sqrt{\frac{2T_1}{M_{\pi p}}}, \tag{2}$$

$$\tau_{nn'} = \frac{l}{v_0^2} \cdot \sqrt{\frac{2T_{nn'}}{M_{\pi p}}}. \tag{3}$$

Here, l is the flight path, $M_{\pi p}$ the mass of the π^-p atom, T_1 the upper kinetic energy limit of the uniform $T_{\pi p}$-distribution, $T_{nn'}$ the kinetic energy of a $\pi^- p$ atom after the Coulomb de-excitation $n \to n'$, and $v_0 = 0.894\,\mathrm{cm/ns}$ the neutron velocity for $\pi^- p$ atoms undergoing charge exchange at rest. It

is assumed that the $\pi^- p$ atoms are not significantly decelerated between Coulomb de-excitation and nuclear capture. Hence, a signature for Coulomb de-excitation would be a step-like structure visible in the TOF-spectra of neutrons from the CEX-reaction.

In our previous experiment [1], the time-resolution of the detector system was not sufficient to resolve a step-like structure in the TOF-spectra. In the present experiment, therefore, several improvements were made in order to be more sensitive to such steps, notably: (i) a reduction in the background, by detecting a γ-ray from π^0-decay, in coincidence with the neutron from the CEX-reaction; (ii) improvement of the time resolution of the neutron detectors by reducing the thickness of both the neutron detecting scintillator and the liquid hydrogen (LH_2) target in the neutron flight-path direction; (iii) improvement in the counting statistics, by an increase of a factor of 15 in the average proton-beam current from the accelerator, as well as improvements to the pion beam optics and a four-fold increase in the neutron detector area. The present experiment was performed at the πE1-channel of PSI; the experimental set-up is shown in Fig. 2.

In the beam counter S1 (see Fig. 2) $3{\cdot}10^5$ negative pions per second at 117 MeV/c were accepted. The pions passed through a carbon degrader, the thickness of which was optimized for a maximal stop rate in the LH_2-target. The hydrogen target had a length of 10 cm in the direction of the pion

beam and 0.5 cm in the direction of the neutron flight path, perpendicular to the pion beam. Neutrons from the hydrogen target were detected after a flight path of variable length (3-12 m) in a detector array consisting of 30 NE102A scintillator disks coupled directly to XP2020 photomultiplier (PM) tubes [12]. These neutrons were accepted only if coincident with a suitably delayed π-stop signal and a γ-ray signal from π^0-decay in an 8×8 matrix of NaI detectors [13].

The two-dimensional scatter plot of the neutron pulse height (analog-to-digital converter, ADC) versus the neutron time-of-flight (time-to-digital converter, TDC) of the raw data from one of the neutron counters is displayed in Fig. 3. The TDC was started with a signal from the neutron counter and stopped by the delayed pion stop signal, hence, the neutron time-of-flight increases to the left. In a first step of the analysis, cuts in the ADC channels were introduced for each neutron counter separately as indicated in Fig. 3, in order to suppress noise events from the photomultipliers (lower ADC cut) and accidental events triggered by photons from π^0-decays or bremsstrahlung from beam electrons (upper ADC cut). Before summing the spectra of all neutron counters, the centre of each neutron peak was shifted by a few TDC channels to channel number 1000. In this way small differences in the transit times of the signals in the PMs and cables as well as small differences in the individual neutron flight paths were corrected for. In the summed spectra

the lower ADC cut was then optimized for a maximal signal-to-noise ratio.

In a second step, cuts were made in the summed photon energy from the NaI wall accepting only events between 60 and 100 MeV. In this way photons from bremsstrahlung and from the $\pi^- p \to \gamma n$ reaction were suppressed. The small remaining accidental background in the TOF spectra was determined and subtracted similarly to the procedure described in Ref[1].

The resulting TOF spectra taken at distances of 4.43 m, 4.73 m and 8.35 m between the LH_2-target and neutron detector are displayed in Fig. 4. In the three spectra an indication for steps was found in the TOF distributions. Their positions, however, did not coincide with those expected from Eq. (1) and (3) for the Coulomb de-excitation process. To our knowledge, no calculations are available at present in which the Coulomb de-excitation process is treated for a collision of a pionic hydrogen atom with a hydrogen *molecule*. It is conceivable, that the de-excitation energy is not simply shared between the pionic atom and a proton but that more complicated processes, involving e.g. molecular break-up or molecular excitations, occur. This would result in deviations from Eq. (1). We therefore decided to treat the positions $T_{nn'}$ of the steps as free parameters in our fit.

The three spectra were fitted simultaneously by TOF distributions, generated by a Monte-Carlo programme[1] which accounted for the intrinsic time resolution and neutron scattering. The fit was restricted to a region from

-15 to $+2$ ns at 4.43 and 4.73 m, and -25 to $+2$ ns at 8.73 m, respectively, to minimize the contributions from scattered neutrons [1]. The free parameters were (a) four energies corresponding to the Coulomb de-excitations from transitions with principal quantum numbers $6 \to 5$, $5 \to 4$, $4 \to 3$, and $3 \to 2$; (b) four yields for the above Coulomb de-excitations; (c) the energy parameter T_1 (cf. Fig. 1a); (d) a distance independent Gaussian time-jitter corresponding to electronic contributions to the time resolution of the apparatus; (e) three normalization factors for the ordinates (events per 0.1 ns), and (f) three shifts to match the time scales of the experimental histograms.

This fit resulted in a χ^2/DOF of 0.99 with 599 degrees of freedom (DOF). The resulting values of the energies $T_{nn'}$ and the relative yields $A_{nn'}$ of the transitions are listed in Table 1. The fitted energies $T_{nn'}$ are lower than the calculated values (Eq. (1)) by the amounts ΔT given in the fourth column of Table 1. The average of the four ΔT values is (-12.7 ± 2.4) eV. The resulting relative yields $A_{nn'}$ agree within a factor of two with those calculated in Ref. [2]. For the low energy component of $f(T_{\pi p})$, our fit resulted in the energy $T_1 = (1.16 \pm 0.14)$ eV and in the yield $A_1 = (45.1 \pm 1.9)$ %.

For comparison, also the old parameterization $f(T_{\pi p})$ which had a first uniform component from 0 to T_1, and a second one from T_1 to T_2, was fitted to the new data. The results of this fit agree with Ref. [1]; however, the χ^2/DOF here is 1.28 (605 DOF) corresponding to a confidence level of

only $4{\cdot}10^{-6}$. In the inserts of the three graphs in Fig. 4, one can see that the experimental distributions tend to form steps, and thus oscillate above and below the fitted curves. In the upper two inserts, the step reaching to the $(3 \rightarrow 2)$ limit ($-10.3\,\mathrm{ns}$ and $-11.0\,\mathrm{ns}$, respectively, corresponding to $T_{\pi p} = 207\,\mathrm{eV}$) is clearly visible.

Conclusions: We have confirmed the existence of strong 'high-energy' components ($T_{\pi p} \gg 1\,\mathrm{eV}$) in the kinetic energy distribution $f(T_{\pi p})$ of $\pi^- p$ atoms in liquid hydrogen at the instant of nuclear $\pi^- p$ capture. These 'high-energy' components contain about half of the $\pi^- p$ atoms. Six percent of the $\pi^- p$ atoms have kinetic energies as high as $\simeq 200\,\mathrm{eV}$. The model of $f(T_{\pi p})$ used in Ref. [1] is inconsistent with the new data. A model which fits the new data is shown in Fig. 1a. The resulting energies $T_{nn'}$(fit) and the yields $A_{nn'}$ are given in the third and fifth columns of Table 1. The resulting parameters for the idealized (uniform) low-energy component of $f(T_{\pi p})$ are $T_1 = (1.16 \pm 0.14)\,\mathrm{eV}$ and $A_1 = (45.1 \pm 1.9)\,\%$. The shape of the 'high energy' components of the $T_{\pi p}$ distribution is close to that derived for Coulomb de-excitation processes. However, the energies $T_{nn'}$ obtained by the fit are significantly lower than those derived from the simplest Coulomb de-excitation model.

We thank Prof. L. I. Ponomarev for fruitful discussions, L. Knecht and

H. Obermeier for their very competent technical assistance, D. Fluri and H. Kind for help during the preparation of the experiment and the data taking, and E. Hermes for help with the neutron detectors. The support from the Hallendienst and many other PSI staff members is gratefully acknowledged. This experiment was supported by the Schweizerischer Nationalfonds zur Förderung der wissenschaftlichen Forschung.

References

[1] J. F. Crawford et al., Phys. Rev. D 43 (1991) 46.

[2] E. C. Aschenauer et al., Phys. Rev. A 51 (1995) 1965.

[3] D. Sigg et al., Phys. Rev. Lett. 75 (1995) 3245, and
D. Chatellard et al., Phys. Rev. Lett. 74 (1995) 4157, and
W. Beer et al., Phys. Lett. B 261 (1991) 16.

[4] V. Markushin, Phys. Rev. A 50 (1994) 1137.

[5] L. Bracci and G. Fiorentini, Nuovo Cimento 43A (1979) 9.

[6] P. Froelich and J. Wallenius, Phys. Rev. Lett. 75 (1995) 2108.

[7] L. I. Men'shikov, Muon Catalyzed Fusion 2 (1988) 173.

[8] W. Czaplinski et al., Muon Catalyzed Fusion 5/6 (1990) 59, and
W. Czaplinski et al., Phys. Rev. A 50 (1994) 525.

[9] L. I. Ponomarev and E. A. Solov'ev, PSI preprint PSI-PR-96-18 (1996),
to be published.

[10] J. F. Crawford et al., PSI Annual Report 1994, Annex I (1995) 32.

[11] R. Frosch, PSI Internal report TM-37-21 (1985), unpublished.

[12] C. Niebuhr et al., Phys. Rev. D 40 (1989) 2796.

[13] A. Bay et al., Nucl. Instr. Meth. in Phys. Res. A271 (1988) 497.

Figure captions

Fig. 1: a) Idealized distribution function $f(T_{\pi p})$ of the kinetic energy $T_{\pi p}$ of pionic hydrogen atoms at the instant of nuclear capture. For clarity, T_1 and the widths of the four δ-like peaks at $T_{nn'}$ are drawn to be 1 eV. The integrals of these peaks correspond to the relative yields A_1 and $A_{nn'}$, respectively. b) Neutron time-of-flight (TOF) distribution $F(\tau)$ corresponding to the kinetic energy distribution of Fig. 1a. Details see text.

Fig. 2: Experimental set-up. 1) central pion trajectory; 2) carbon degrader; 3) scintillator S1; 4) liquid hydrogen target (LH_2); 5) vacuum vessel of the LH_2-target; 6) CH_2-collimator; 7) concrete shielding; 8) central neutron trajectory; 9) lead collimator; 10) neutron detection scintillators S_{ni}, $i = 1, 30$; material NE102A, thickness 5 mm, diameter 45 mm. 11) XP2020 photomultiplier tubes; 12) NaI crystals (8×8 matrix) for the detection of photons from π^0-decay.

Fig. 3: Two-dimensional event distribution recorded at a distance of $l = 4.73$ m between the LH_2-target and the neutron detector array. Abscissa: relative neutron time-of-flight for one neutron counter; 1 ns corresponds to 10 TDC channels; time increases to the left. Ordinate: neutron pulse height.

Fig. 4: Histograms: measured time-of-flight spectra of neutrons from the charge exchange reaction $\pi^- p \to \pi^0 n$, after background subtraction, for flight paths of 4.43 m, 4.73 m, and 8.35 m. Time is measured from the centre of the neutron peak corresponding to $v_0 = 0.894\,\mathrm{cm/ns}$ [1]. Curves: fits to the data including Coulomb de-excitation processes. The numbers $n \to n'$ indicate the fitted positions of the steps in the TOF distribution of neutrons which are emitted after the corresponding Coulomb de-excitation. For comparison, the fit using the parameterization of Ref. [1] (two uniform kinetic-energy distributions of the $\pi^- p$ atoms) is shown in the inserts.

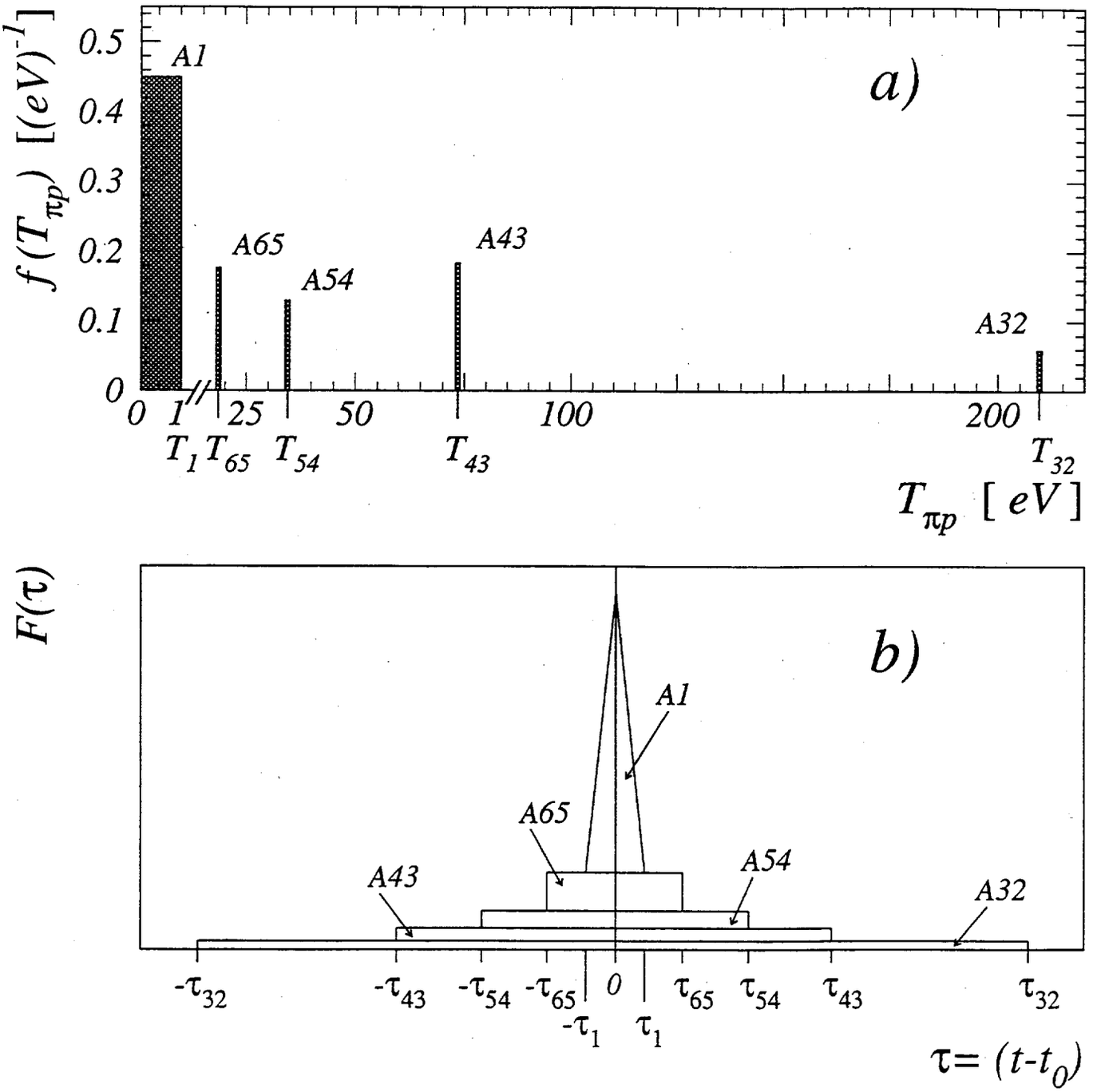
a)
$f(T_{\pi p})\ [(eV)^{-1}]$
0.5
0.4
0.3
0.2
0.1
0
A1
A65
A54
A43
A32
0
1
25
50
100
200
T_1
T_{65}
T_{54}
T_{43}
T_{32}
$T_{\pi p}$ [eV]
b)
$F(\tau)$
A1
A65
A43
A54
A32
$-\tau_{32}$
$-\tau_{43}$
$-\tau_{54}$
$-\tau_{65}$
$-\tau_1$
0
τ_1
τ_{65}
τ_{54}
τ_{43}
τ_{32}
$\tau = (t-t_0)$

Fig. 1

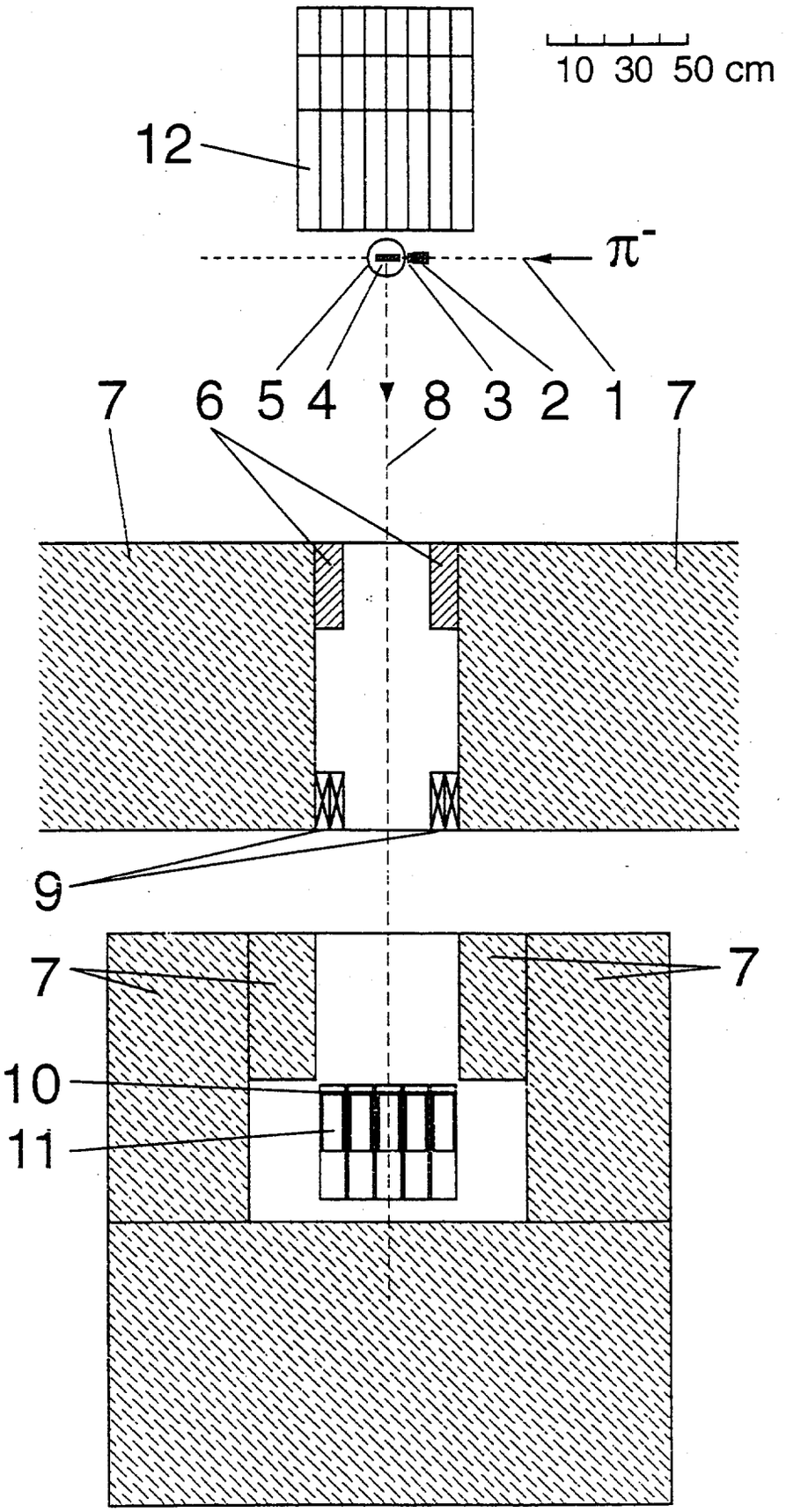

Fig. 2

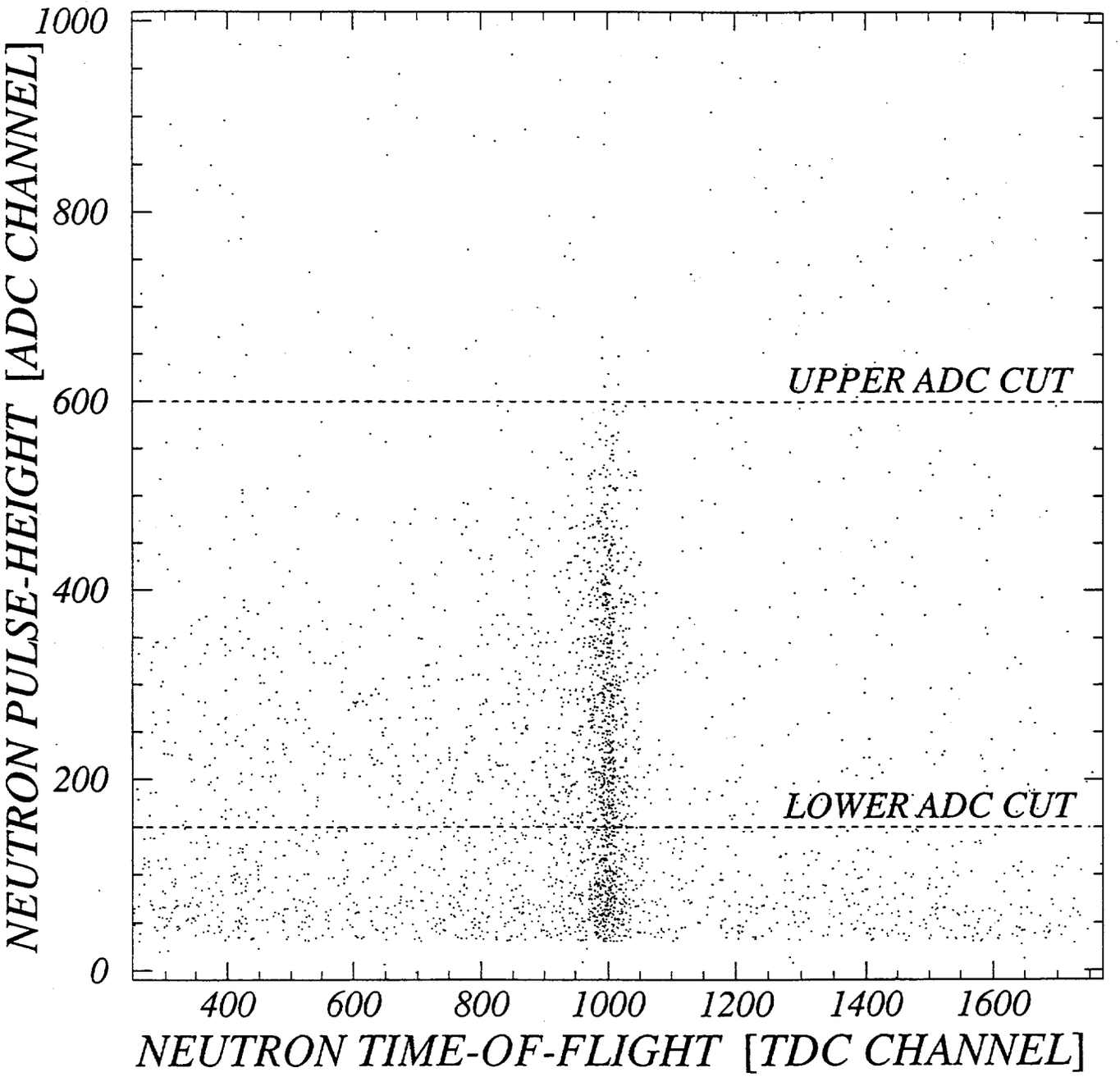
1000
800
600
400
200
0
NEUTRON PULSE-HEIGHT [ADC CHANNEL]
UPPER ADC CUT
LOWER ADC CUT
400
600
800
1000
1200
1400
1600
NEUTRON TIME-OF-FLIGHT [TDC CHANNEL]

Fig. 3

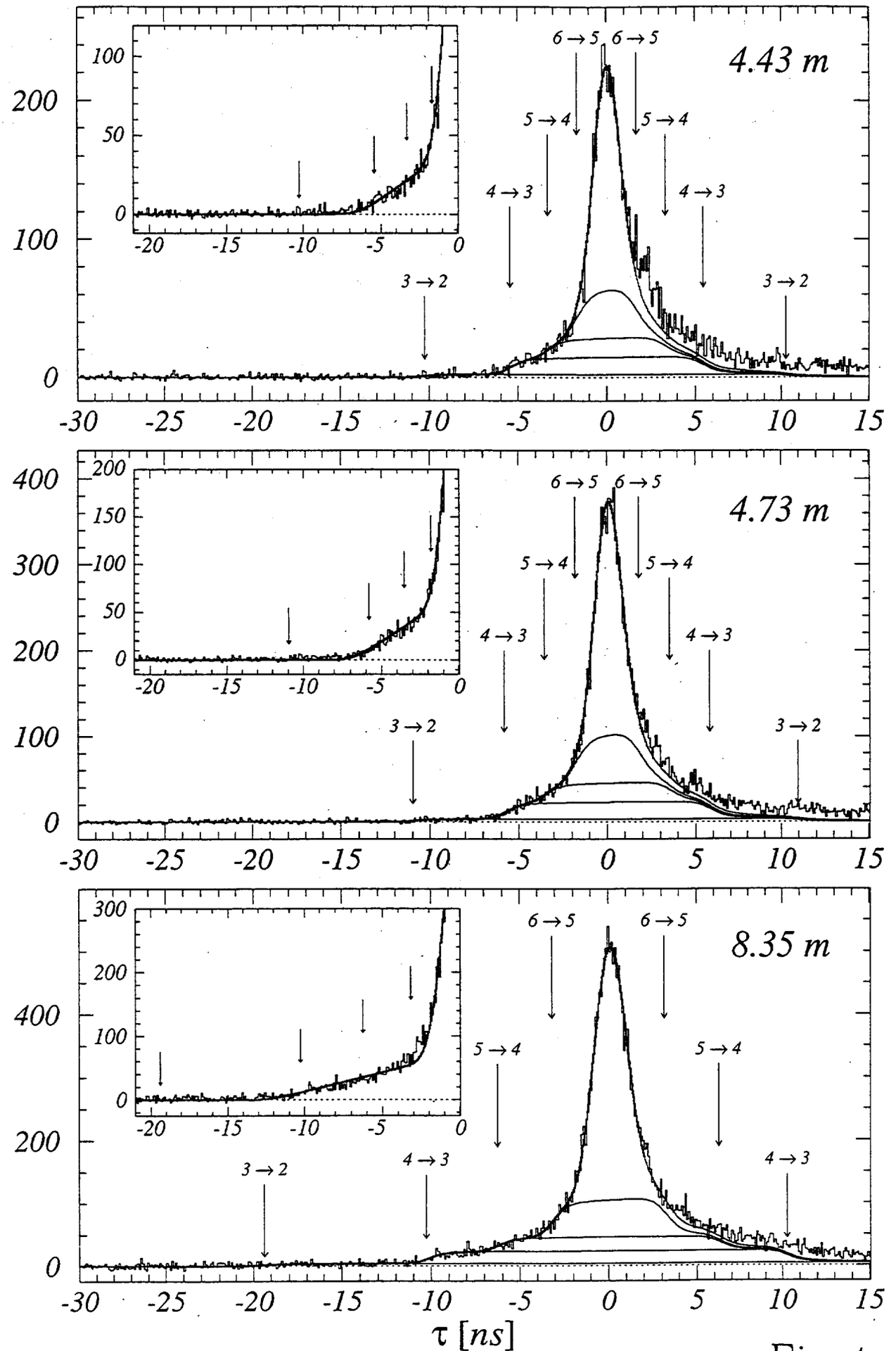

Fig. 4

Transition	$T_{nn'}$(calc.)[eV]	$T_{nn'}$(fit)[eV]	ΔT [eV]	yield $A_{nn'}$ [%]
6→5	18.4	5.6±2.8	−12.8±2.8	17.6±2.1
5→4	33.9	21.7±5.5	−12.2±5.5	13.0±1.7
4→3	73.2	57.2±9.0	−16.0±9.0	18.4±1.5
3→2	209.1	207±19	−2±19	5.9±0.7

Table 1: Calculated (Eq.(1)) and fitted kinetic energies $T_{nn'}$ and fitted yields $A_{nn'}$ of Coulomb de-excitation peaks in the kinetic energy distribution $f(T_{\pi p})$; cf. Fig. 1a. Column 4 gives $\Delta T = T_{nn'}(\text{fit}) - T_{nn'}(\text{calc.})$.